Electronic Supplementary Material (ESI) for Inorganic Chemistry Frontiers.

A new TIFSIX anion pillared metal organic framework with abundant electronegative sites for efficient C_2H_2/CO_2 separation

Nuo Xu,[a§] Tongan Yan,[b§] Jiahao Li,[a§] Lingyao Wang,[a*] Dahuan Liu,[b] Yuanbin Zhang[a*]

[a] *Key Laboratory of the Ministry of Education for Advanced Catalysis Materials, College of Chemistry and Life Sciences, Zhejiang Normal University, Jinhua 321004, China.*

E-mail: ybzhang@zjnu.edu.cn; lywang@zjnu.edu.cn

[b] *State Key Laboratory of Organic-Inorganic Composites, Beijing University of Chemical Technology, Beijing 100029, China*

[§] *These authors contributed equally to this work.*

I. General Information and Procedures

Chemicals: 1,2-Di(4-pyridyl)ethylene was purchased from Energy Chemical without further purification. $Cu(NO_3)_2 \cdot 3H_2O$ was purchased from Macklin. $(NH_4)_2TiF_6$ was purchased from Alab Chemical Technology. C_2H_2 (99.5%), CO_2 (99.9%) and C_2H_2/CO_2 (50:50) were purchased from Datong Co., Ltd. (Jinhua). All reagents and solvents were used as received without further purification.

Preparation of single crystals of ZNU-7: To a 5 mL long thin tube was added a 1 mL of aqueous solution with $(NH_4)_2TiF_6$ (1 mg) and $Cu(NO_3)_2 \cdot 3H_2O$ (1 mg). 1 mL of MeOH/H_2O mixture was slowly layered above the solution, followed by a 1 mL of MeOH solution, and 1 mL of MeOH solution of 1,2-Di(4-pyridyl)ethylene(2 mg) was added to the top. The tube was sealed and left undisturbed at RT. After several days, blue flake shaped crystals were formed on the glass surface. The average yield is ca 60% .

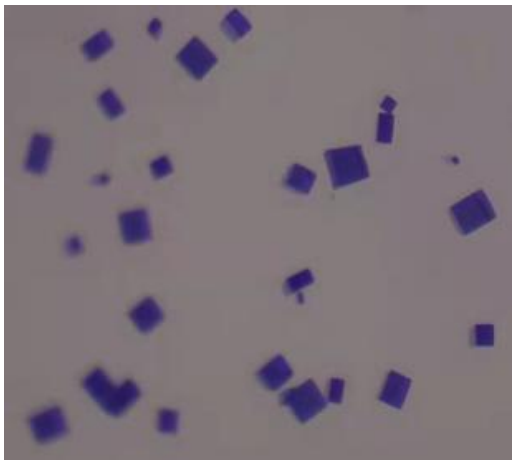

Fig. S1. The microscopic image of as-synthesized **ZNU-7**.

Single-crystal X-ray diffraction studies were conducted at 193 K on the BrukerAXS D8 VENTURE diffractometer equipped with a PHOTON-100/CMOS detector (GaKα, λ = 1.34139 Å). Indexing was performed using APEX2. Data integration and reduction were completed using SaintPlus 6.01. Absorption correction was performed by the multi-scan method implemented in SADABS. The space group was determined

using XPREP implemented in APEX2.1 The structure was solved with SHELXS-97 (direct methods) and refined on F2 (nonlinear least-squares method) with SHELXL-97 contained in APEX2, WinGX v1.70.01, and OLEX2 v1.1.5 program packages. All non-hydrogen atoms were refined anisotropically. The contribution of disordered solvent molecules was treated as diffuse using the Squeeze routine implemented in Platon.

Powder X-ray diffraction (PXRD) data were collected on a SHIMADZU XRD-6000 diffractometer (Cu Kαλ = 1.540598 Å) with an operating power of 40 KV, 30 mA and a scan speed of 4.0°/min. The range of 2θ was from 5° to 50°.

Thermal gravimetric analysis was performed on a TGA Q500 V20.13 Build 39 instrument. Experiments were carried out using a platinum pan under nitrogen atmosphere which conducted by a flow rate of 60 mL/min nitrogen gas. The data were collected at the temperature range of 50 °C to 600 °C with a ramp of 10 °C /min.

The gas adsorption measurements were performed on a 3H-2000PS2 instrument (Beishide Instrument Technology (Beijing) Co., Ltd.) for N_2 and on a Builder SSA 7000 instrument (Beijing Builder Electronic Technology, Co., Ltd) for C_2H_2, CO_2 and C_2H_4. Before gas adsorption measurements, the sample of ZNU-7 was evacuated at 25 ^{o} C for 2 hours firstly, and then at 75 ^{o} C for 12 h. The adsorption isotherms were collected at 77, 278 , 298 and 308 K on activated samples. The experimental temperatures were controlled by liquid nitrogen bath (77 K) and water bath (278 , 298 and 308 K), respectively.

Fitting of experimental data on pure component isotherms

The unary isotherm data for CO_2 measured at three different temperatures 278 , 298 and 308 K in ZNU-7 were fitted with good accuracy using the single-site Langmuir model, where we distinguish one adsorption sites A:

$$q = \frac{q_{sat,A} b_A p}{1 + b_A p} \tag{S1}$$

The unary isotherm data for C_2H_2 measured at three different temperatures 278 , 298 and 308 K in ZNU-7 were fitted with good accuracy using the dual-site Langmuir model, where we distinguish two distinct adsorption sites A and B:

$$q = \frac{q_{sat,A} b_A p}{1 + b_A p} + \frac{q_{sat,B} b_B p}{1 + b_B p} \tag{S2}$$

Here, P is the pressure of the bulk gas at equilibrium with the adsorbed phase (Pa), q is the adsorbed amount per mass of adsorbent (mol kg^{-1}), $q_{sat,\,A}$ and $q_{sat,\,B}$ are the saturation capacities of site A and B (mol kg^{-1}), b_A and b_B are the affinity coefficients of site A and B (Pa^{-1}).

In eq (S3), the Langmuir parameters b_A, b_B can be temperature dependent or temperature independent .

$$b_A = b_{A0} \exp\left(\frac{E_A}{RT}\right); \quad b_B = b_{B0} \exp\left(\frac{E_B}{RT}\right) \tag{S3}$$

In eq (S3), E_A, E_B are the energy parameters associated with sites A, and B, respectively.

The isosteric heat of adsorption, Q_{st}, is defined as

$$Q_{st} = -RT^2 \left(\frac{\partial \ln p}{\partial T}\right)_q \tag{S4}$$

where the derivative in the right member of eq (S5) is determined at constant adsorbate loading, q. The calculations are based on the use of the Clausius-Clapeyron equation.

IAST calculations of adsorption selectivity

The IAST adsorption selectivity for two gases is defined as:

$$S_{ads} = \frac{q_1/q_2}{p_1/p_2} \quad \text{(S5)}$$

q_1, and q_2 are the molar loadings in the adsorbed phase in equilibrium with the bulk gas phase with partial pressures p_1, and p_2.

Breakthrough experiments

The breakthrough experiments were carried out on a dynamic gas breakthrough equipment HPMC-41 (Xuzhou North Gaorui Electronic Equipment Co., Ltd). The experiments were conducted using a stainless steel column (4.6 mm inner diameter × 50 mm length). The weight of ZNU-7 powder packed in the columns were 0.399 g. The column packed with ZNU-7 was first purged with a Ar flow (5 mL min^{-1}) for 12 h at 50 °C. The mixed gas of C_2H_2/CO_2 (50/50, v/v/) was then introduced. Outlet gas from the column was monitored using gas chromatography (GC-9860-5CNJ) with the thermal conductivity detector TCD. After the breakthrough experiment, the sample was regenerated with a Ar flow of 5 mL min^{-1} under 75 °C for 12 h.

Calculation of separation factor (α)

The amount of gas adsorbed i (q_i) is calculated from the breakthrough curve using the following:

$$q_i = \frac{V_T P_i \Delta T}{m} \quad \text{(S6)}$$

Here, V_T is the total flow rate of gas (cm^3/min), P_i is the partial pressure of gas i (atm), ΔT is the time for initial breakthrough of gas i to occur (mins) and m is the mass of the sorbent (g). The separation factor (α**)** of the breakthrough experiment is determined as

$$\alpha = \frac{q_1 y_2}{q_2 y_1} \quad \text{(S7)}$$

Where, y_i is the partial pressure of gas i in the gas mixture.

Simulation Details

In the RASPA package (Mol. Simul. 2016, 42, 81−101.), the adsorption process of C_2H_2 and CO_2 was simulated by grand canonical Monte Carlo (GCMC) method. Van der Waals force (vdW) and Coulomb potential interactions between the framework

and adsorbed molecules were considered in the simulation process. The Lennard-Jones (LJ) equation was used to describe dispersive interactions and its parameters were calculated by the Lorentz-Berthelot mixed rule. In all simulations, the framework was assumed rigid (i.e. atoms were frozen in the positions determined by crystal structure determination) and the partial point charge were distributed according to the QEq method (Chem. Eng. J., 2011, 171, 775–781.) using Wells et al's code (J. Phys. Chem. C, 2015, 119, 456–466.).

For the framework, the LJ parameters of the metal atoms were taken from the UFF force field (J. Am. Chem. Soc. 1992, 114 (25), 10024−10035.) while those of the other elements were taken from the DREIDING force field (J. Phys. Chem. 1990, 94, 8897−8909).

A rigid three-point charged LJ linear model was used for C_2H_2 and CO_2. C_2H_2 was treated as a four-site model with the LJ positions located on the carbon atoms from the work by Fischer *et al.* (ChemPhysChem 2010, 11, 2220–2229). The C–C and C–H bond lengths are 1.2111 and 1.0712 Å, respectively. The partial point charges centered at each site are q_C = −0.278 e and q_H = 0.278 e. A rigid three-point charged LJ linear model was used for CO_2. The energy parameters of CO_2 were taken from the TraPPE force field (J. Phys. Chem. B 1998, 102 (14), 2569−2577.), and the C–O bond length was set at 1.149 Å. Partial point charges centered at each LJ site are q_O = −0.35 e and q_C = 0.70 e.

The number of ZNU-7 unit cell in the simulation box was 2×2×4 to ensure that the simulation unit was extended to be at least 28.0 Å along each dimension. Periodic boundary conditions were applied. The dispersive interactions were calculated using a long-range correction with a spherical cut-off radius of 14.0 Å, while the Ewald sum was used to consider the electrostatic interactions. The Peng-Robinson equation of state was used to convert the fugacity. In order to determine the preferential adsorption sites of guest molecules in the material, Monte Carlo simulation in the canonical ensemble (NVT-MC) was firstly performed to obtain the center of mass (COM) probability distributions of adsorbate molecules in the identified MOF. 50000 cycles of GCMC simulations were performed, including 25000 equilibrium cycles

and 25000 ensemble average cycles. In each cycle, the adsorbed molecules underwent three types of trials: translation, rotation and regeneration. Further increasing the number of cycles had no significant effect on the adsorption results.

Theoretical Calculations

Geometric optimization of guest molecules in MOFs was performed using density functional theory (DFT) method in Dmol^3 of Materials Studio. Generalized gradient approximation (GGA) with the Perdew-Burke-Ernzerh (PBE) of functional was applied for the calculations, combining the double numerical plus d-functions (DND) basis set. Self-consistent field (SCF) calculations were carried out with the convergence criterion of 10^{-5} Ha in energy. To accelerate SCF convergence, thermal smearing was used with a value of 0.005 Ha to orbital occupation.

The static binding energy E_b for each binding site was calculated by the following equation:

$$E_b=E_{gas+MOF}-E_{MOF}-E_{gas} \quad \text{(S8)}$$

where $E_{gas+MOF}$ stands for the energy of the optimized gas-MOF complex, E_{MOF} and E_{gas} are the energies of the optimized bare framework and the isolated adsorbate molecule, respectively.

II Characterization (SCXRD, PXRD, TGA)

Table S1. Crystallographic data for ZNU-7.

Compounds	**ZNU-7**
Moiety formula	C_{24} H_{20} Cu F_6 N_4 Ti
Temperature（K）	193
Space group	P4/n
a(Å)	18.8668(15)
b(Å)	18.8668(15)
c(Å)	c = 8.3590(7)
α(deg)	90
β(deg)	90
γ(deg)	90
Volume($Å^3$)	2975.4(5)
Z	2
Dx(g cm^{-3})	0.658
Mu (mm^{-1})	2.866
$F_{(000)}$	594
R	0.1621
wR_2	0.3467

$R_1=\Sigma||F_o|-|F_c||/\Sigma|F_o|$, $wR_2= |\Sigma w(|F_o|^2-|Fc|^2)|/\Sigma|w(Fo^2)^2|^{1/2}$

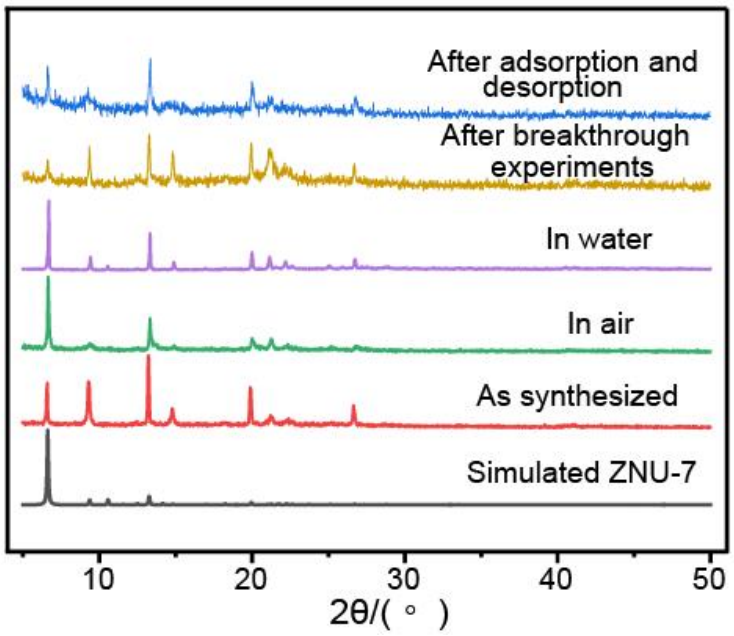

Fig. S2 PXRD patterns of ZNU-7 under different treatments.

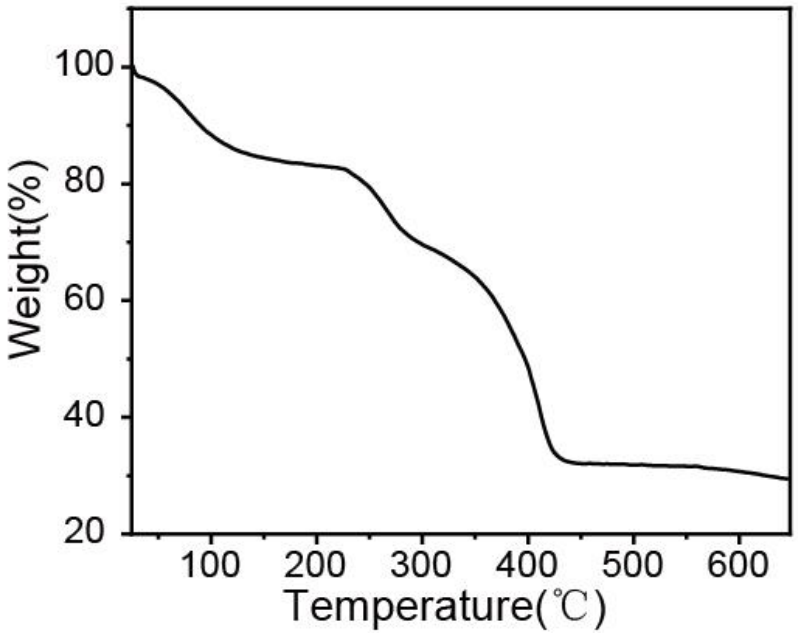

Fig. S3 TGA curves of ZNU-7.

III Adsorption data

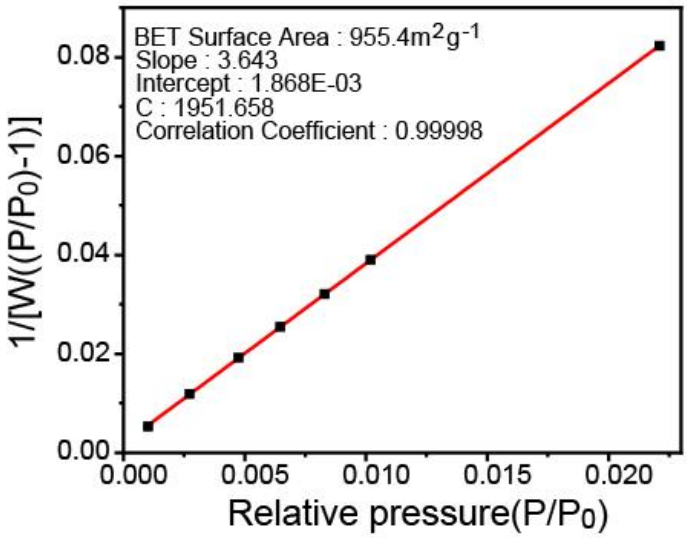

Fig. S4 BET surface area plot of ZNU-7.

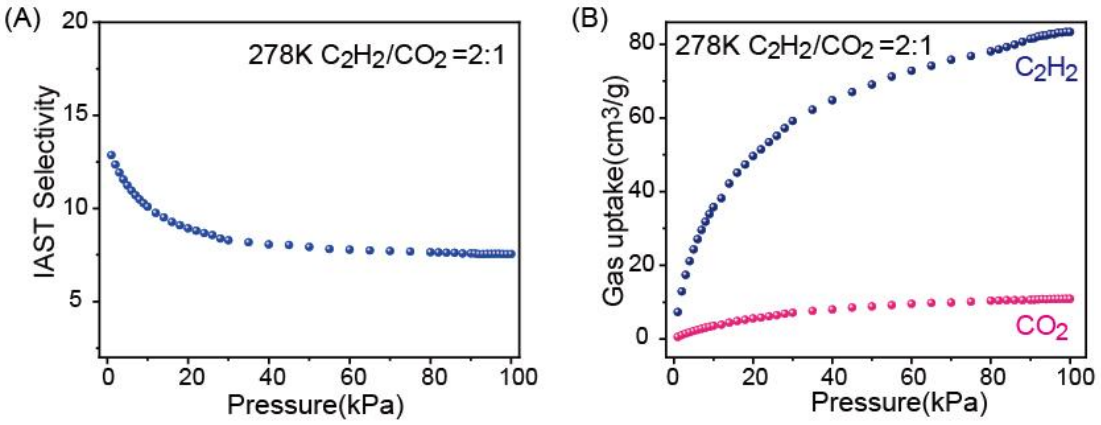

Fig. S5 (A) IAST selectivity for C_2H_2/CO_2 (2:1) mixture in ZNU-7 at 278 K. **(B)** The adsorption isotherm of C_2H_2 and CO_2 from C_2H_2/CO_2 (2:1) mixture at 278 K on ZNU-7 based on IAST calculation.

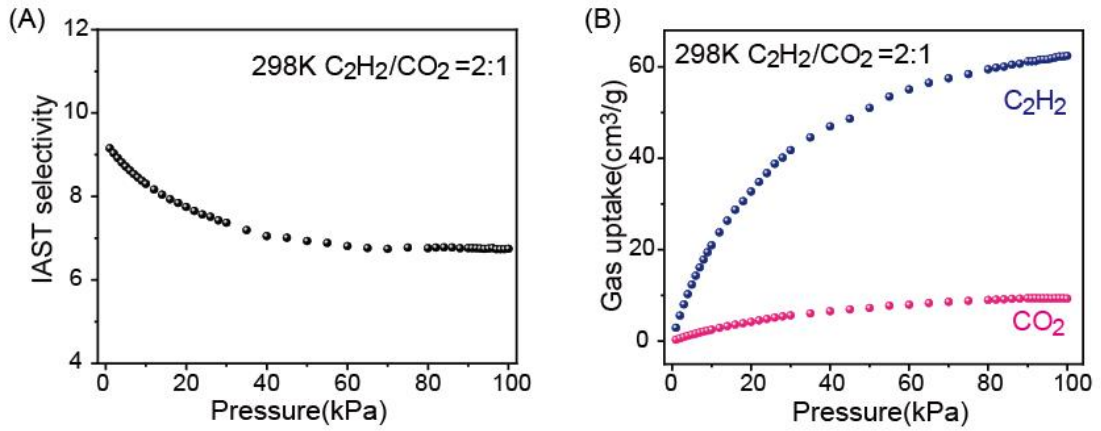

Fig. S6 (A) IAST selectivity for C_2H_2/CO_2 (2:1) mixture in ZNU-7 at 298K. **(B)** The adsorption isotherm of C_2H_2 and CO_2 from C_2H_2/CO_2 (2:1) mixture at 298 K on ZNU-7 based on IAST calculation.

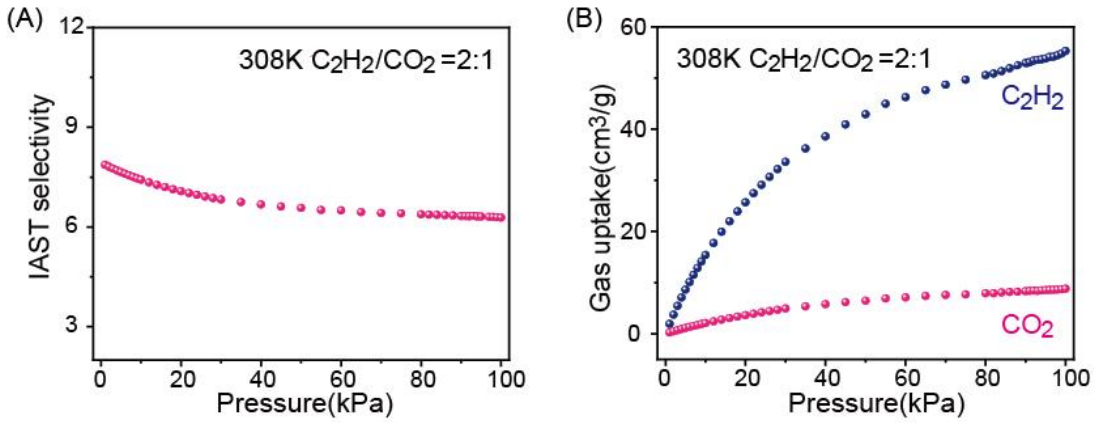

Fig. S7 (A) IAST selectivity for C_2H_2/CO_2 (2:1) mixture in ZNU-7 at 308 K. **(B)** The adsorption isotherm of C_2H_2 and CO_2 from C_2H_2/CO_2 (2:1) mixture at 308 K on ZNU-7 based on IAST calculation.

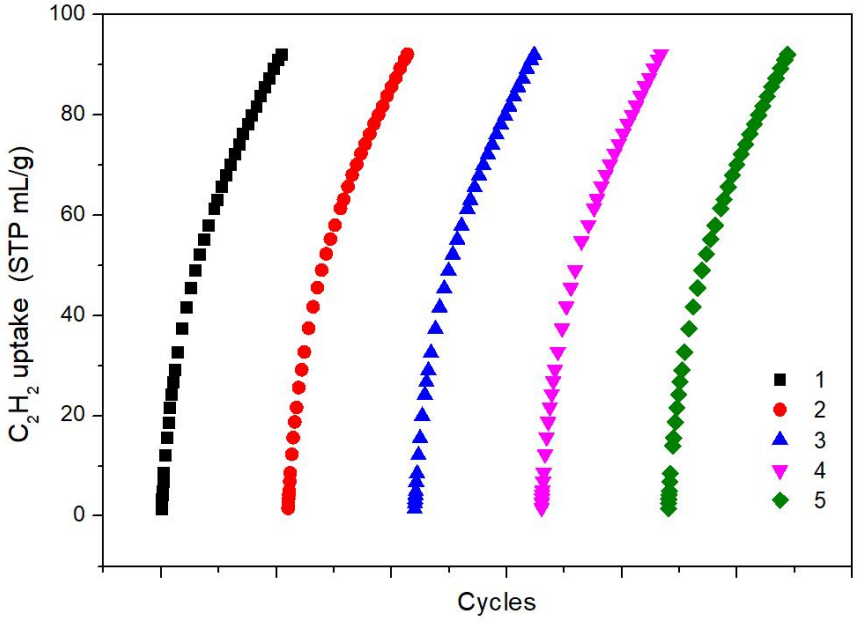

Fig. S8 Five cycles of C_2H_2 adsorption isotherms

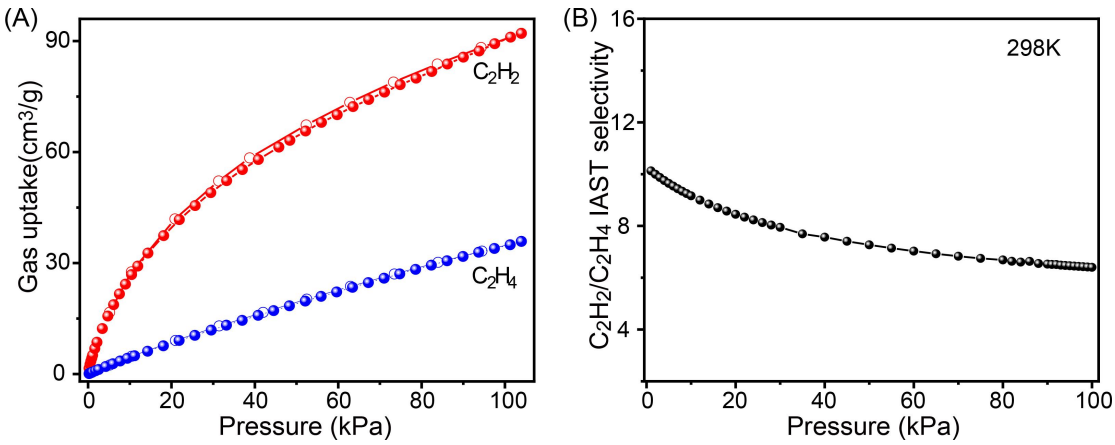

Fig. S9 (A) C_2H_2 and C_2H_4 adsorption and desorption isotherms at 298 K. (B) IAST selectivity for C_2H_2/C_2H_4 (1:1) mixture in ZNU-7 at 298 K. The adsorption capacity of C_2H_4 is only 35.9 cm^3/g at 298 K and 1 bar. Further IAST calculation shows that the selectivity of C_2H_2/C_2H_4 is 10.1-6.4, suggesting ZNU-7 is possible to separate C_2H_2/C_2H_4 efficiently.

Table S2. Q_{st} and $\Delta Q_{st}(C_2H_2\text{-}CO_2)$ for popular C_2H_2/CO_2 separation physisorbents.

Adsorbent	Q_{st} C_2H_2 (kJ/mol)	Q_{st} CO_2 (kJ/mol)	Δq
ZNU-7	35.3	22.5	12.8
UTSA-50	39.4	27.8	11.6
TCuCl	41	30.1	10.9
PCP-32	36	26	10
BSF-1	30.7	21.7	9
BSF-2	37.3	28.7	8.6
JXNU-12(F)	28	19.7	8.3
CAU-23	26.7	20	6.7
CAU-10-NH_2	31.3	24.5	6.8
NbU-10	34.6	27.6	7
SNNU-150-Al	29	24.8	4.2
Cu-CPAH	35.4	31.5	3.9
DICRO-4-Ni-i	37.7	33.9	3.8
FJU-89a	31	27.8	3.2
NTU-55	25.5	22	3.5
JCM-1	36.9	33.4	3.5
PCP-33	27.5	26	1.5
SNNU-37(Sc)	34.4	33.4	1
ZJUT-2a	41.5	35.5	6
SNNU-150-Ga	33.0	28.0	5

Table S3. Parameter fits for C_2H_2 and CO_2 in ZNU-7.

	Site A			Site B			Correlation Coefficient R^2
Parameter	$q_{A,sat}$	B_{A0}	E_A	$q_{B,sat}$	B_{B0}	E_B	
unit	mL/g	Pa^{-VA}	(kJ/mol)	mL/g	Pa^{-1}	kJ/mol	
C_2H_2	164.94	9.33E-07	21.23	39.57	2.07E-08	37.88	0.999761
CO_2	132.22	4.03E-07	22.52	--	--	--	0.999404

Table S4 Comparison of the reported materials on C_2H_2/CO_2 adsorption capacity, adsorption enthalpy (Q_{st}), IAST selectivity of C_2H_2/CO_2 and C_2H_2/CO_2 uptake ratio.

Porous Materials	C_2H_2 uptake (cm^3/g)	CO_2 uptake (cm^3/g)	Q_{st} (C_2H_2) (kJ/mol)	Q_{st} (CO_2) (kJ/mol)	IAST selectivity	C_2H_2/CO_2 uptake ratio	Ref
C_2H_2/CO_2 adsorption by thermodynamic mechanism							
CAU-10-H	89.8	60	27	25	4	1.5	[1]
Cu@UiO-66-$(COOH)_2$	51.7	20	74.5	28.9	73*	2.58	[2]
JCM-1	75	38	36.9	33.4	13.7	1.97	[3]
NKMOF-1-Ni	61	51.1	60.3	40.9	26	1.19	[4]
FJU-90	180	103	25.1	20.7	4.3	1.75	[5]
MAF-2	70.1	19.04	29.8	25.8	N.A.	3.68	[7]
NTU-66-Cu	111.5	49	32.3	21.7	6	2,27	[8]
iMOF-5C	32.48	14.56	35.5	N.A.	6	2.23	[9]
iMOF-6C	24.86	13.22	38	N.A.	8	1.17	[9]
iMOF-7C	15.68	13.66	35	N.A.	4	1.15	[9]
MIL-160	190.85	90.05	31.8	26.9	10	2.12	[10]
CAU-23	118.9	71.9	26.7	20	3.8	1.65	[10]
ZJU-60	150	73.9	17.6	15.2	6.7[a]	2.05	[11]
UTSA-68a	70.1	39.6	25.8	26	3.4[b]	1.77	[12]
JXNU-5a	55.9	34.8	32.9	25.2	5	1.61	[13]
FeNi-M'MOF	96	60.9	27	24.5	24	1.58	[14]
SNNU-150-In	153.2	56	23.4	24,9	7	1.51	[15]
SNNU-150-Al	97	44.4	29	24	7.27	2.18	[15]
FJU-36a	52.2	35.5	32.9	31.1	2.8	1.47	[16]
Cu(BDC-Br)	34.3	24.2	26.1	25.6	3.9	1.42	[17]
TCuI	49.3	35.8	38.4	30.7	5.3	1.375	[18]
TCuCl	67.2	44.8	41	30.1	16.9	1.5	[18]
TCuBr	62.7	44.8	36.8	26.8	9.5	1.4	[18]
SNNU-45	133.95	97.44	39.9	27.1	8.5	1.37	[19]

SNNU-63	91.1	43.7	21.6	21.9	2.7	2.08	[20]
SNNU-65-Cu-Sc	178.9	70.4	44.9	22.2	13.5	2.5	[21]
SNNU-65-Cu-Fe	162.3	64.9	28.2	21.8	6.7	2.5	[21]
ZJU-74a	85.7	69	44.5	30	36.5	1.25	[22]
ATC-Cu	112.2	90.05	79.1	N.A.	53.6	1.25	[23]
JNU-1	61.6	50.4	13	24	3	1.2	[24]
MUF-17	67.4[f]	56.2[f]	49.5	33.8	6[f]	1.2	[25]
PCM-48	25.54	21.73	26.3	15.4	4.3	1.175	[26]
SIXSIF-Cu-TPA	185.2	107.3	39.1	25.7	5.2	1.06	[27]
UTSA-74a	107	71	31.7	25	9	1.5	[28]
PCP-33	121.8	58.6	27.5	26.2	6	2.08	[29]
NTU-55	135.5	70	25	22	6.6[a]	1.94	[30]
ZJU-199	128	62.4	38.5	19	4[b]	2.05	[31]
UPC-200(Al)-F-BIM	144.5	55.5	20.5	14.2	3.15	2.6	[32]
ZJU-195a	214.2	105	29.9	20.7	4.7	2.04	[33]
ZJNU-13	118.4	87.9	33.5	22.5	5.64	1.35	[34]
DICRO-4--Ni-i	43	23	37.7	33.9	13.9	1.87	[35]
$Ni_3(HCOO)_6$	94	68	40.9	24.5	22	1.38	[36]
ZJUT-2	76[b]	49[b]	41.5	31.5	10[b]	1.55	[37]
BSF-1	52.5	39.7	30.7	21.7	3.4	1.32	[38]
BSF-2	41.5	29.7	37.3	28.7	5.1	1.4	[39]
BSF-3	81.7	47.3	42.7	25.5	16.3	1.73	[40]
BSF-3-Co	86.2	54	N.A.	N.A.	12.7	1.67	[40]
BSF-4	53.2	35.8	35.0	24.5	9.8	1.5	[41]
BSF-9(ZNU-1)	76.3	38.1	54.0	44.0	56.6	2.0	[42]
BSF-10	65	25.8	34.8	22.9	5.86	2.52	[43]
ZNU-7	**92.1**	**36.0**	**35.3**	**22.5**	**6.6**	**2.6**	**This work**
C_2H_2/CO_2 adsorption by molecular sieving mechanism							
UTSA-300	68.9	3.36	57.6	N.A.	743	20.5	[44]

ZNU-3	81	5.44	23.4	N.A.	N.A.	14.9	[45]
SIFSIX-dps-Cu	102.3	13.66	60.5	N.A.	1786.6	7.5	[46]
GeFSIX-dps-Cu	90.5	10.08	56.3	N.A.	171.9	8.98	[46]
NTU-65	75.26	2.24	N.A.	N.A.	N.A.	33.6	[47]
CPL-1-NH_2	41.2	4.7	50	32.4	119	8.76	[48]

[a] IAST selectivity at 0.15 bar for 1 : 1 (v/v) C_2H_2/CO_2. [b] At 296 K. [c] At 273 K. [d] At 270 K. [e] Uptake ratio at 0.01 bar and 270 K. [f] At 293 K. [g] at 288 K. [h] at 308 K

N.A. = not available.

* The reported value of 185 in Ref 24 is the IAST selectivity under 273 K (see Figure S29 in Ref. 24) while the IAST selectivity for C_2H_2/CO_2 (1/1) at 298 K is ~73

IV Modeling study

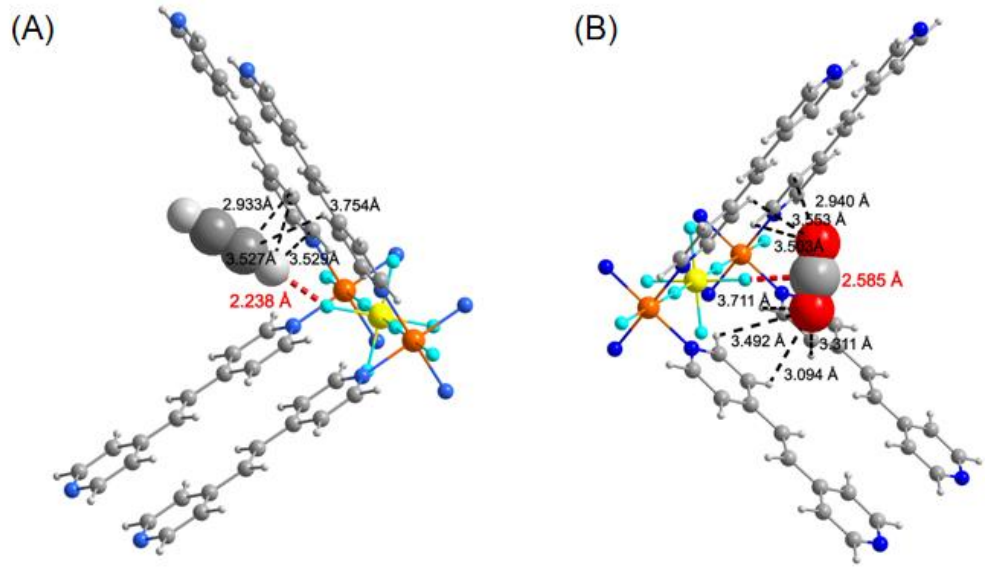

Fig. S10 (A) Host-guest interactions between C_2H_2 and ZNU-7; **(B)** Host-guest interactions between CO_2 and ZNU-7.

V Breakthrough experiments

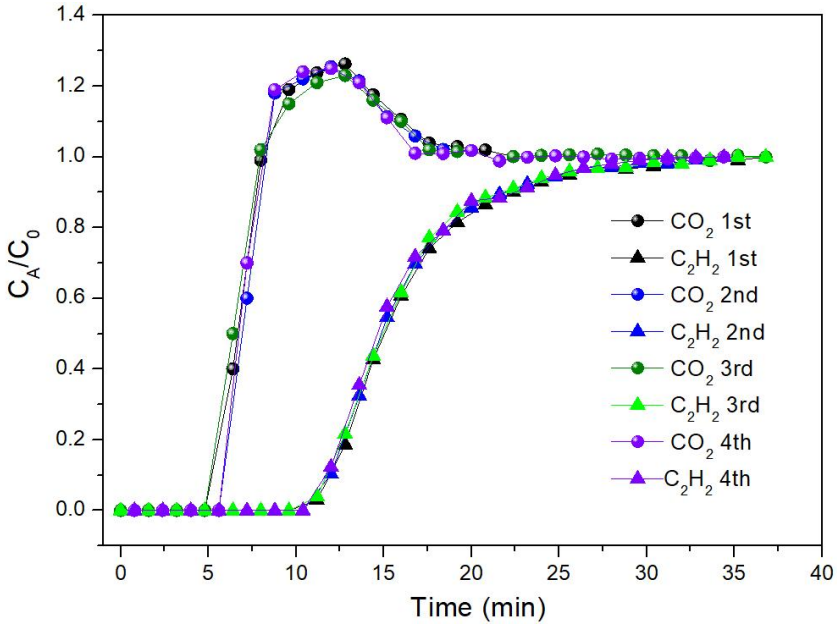

Fig. S11 Four cycles of C_2H_2/CO_2 (1/1) breakthrough experiments with a total flowrate of 2.5 mL/min at 298K for ZNU-7.

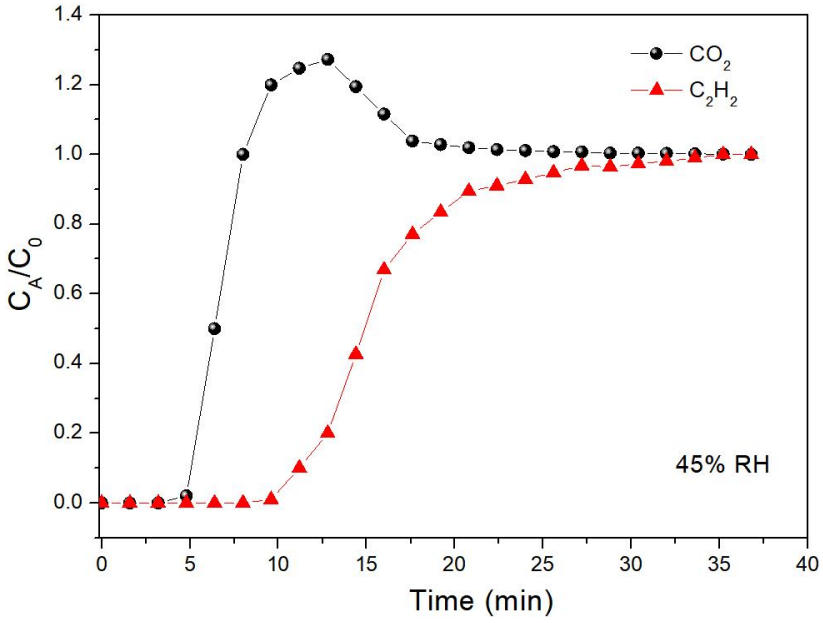

Fig. S12 The C_2H_2/CO_2 (1/1) breakthrough experiment with a total flowrate of 2.5 mL/min at 298K under humid condition (45% RH) for ZNU-7.

Reference

[1] J. Pei, H. Wen, X. Gu, Q. Qian, Y. Yang, Y. Cui, B. Li, B. Chen and G. Qian, Dense Packing of Acetylene in a Stable and Low-Cost Metal-Organic Framework for Efficient C_2H_2/CO_2 Separation, *Angew. Chem. Int. Ed*. 2021, **60**, 25068-25074.

[2] L. Zhang, K. Jiang, L. Yang, L. Li, E. Hu, L. Yang, K. Shao, H. Xing, Y. Cui, Y. Yang, B. Li, B. Chen and G. Qian, Benchmark C_2H_2/CO_2 Separation in an Ultra-Microporous Metal–Organic Framework via Copper(I)-Alkynyl Chemistry, *Angew. Chem. Int. Ed.* 2021, **60**, 15995-16002.

[3] J. Lee, C. Y. Chuah, J. Kim, Y. Kim, N. Ko, Y. Seo, K. Kim, T. H. Bae and E. Lee, Separation of Acetylene from Carbon Dioxide and Ethylene by a Water-Stable Microporous Metal-Organic Framework with Aligned Imidazolium Groups inside the Channels, *Angew. Chem. Int. Ed*., 2018, **57**, 7869-7873.

[4] Y. Peng, T. Pham, P. Li, T. Wang, Y. Chen, K. Chen, K. Forrest, B. Space, P. Cheng, M. Zaworotko and Z. Zhang, Robust Ultramicroporous Metal-Organic Frameworks with Benchmark Affinity for Acetylene, *Angew. Chem., Int. Ed.*, 2018, **57**, 10971-10975.

[5] Y. Ye, Z. Ma, R. Lin, R. Krishna, W. Zhou, Q. Lin, Z. Zhang, S. Xiang and B. Chen, Pore Space Partition within a Metal-Organic Framework for Highly Efficient C_2H_2/CO_2 Separation, *J. Am. Chem. Soc*., 2019, **141**, 4130-4136.

[6] P. Li, Y. He, Y. Zhao, L. Weng, H. Wang, R. Krishna, H. Wu, W. Zhou, Y. Han and B. Chen, A Rod-Packing Microporous Hydrogen-Bonded Organic Framework for Highly Selective Separation of C_2H_2/CO_2 at Room Temperature. *Angew. Chem. Int. Ed.*, 2015, **127**, 584-587.

[7] J. Zhang and X. Chen, Optimized Acetylene/Carbon Dioxide Sorption in a Dynamic Porous Crystal*, J. Am. Chem. Soc.*, 2019, **131**, 5516-5521.

[8] S. Chen, N. Behera, C. Yang, Q. Dong, B. Zheng, Y. Li, Q. Tang, Z. Wang, Y. Wang and J. Duan, A chemically stable nanoporous coordination polymer with fixed and free Cu^{2+} ions for boosted C_2H_2/CO_2 separation, *Nano Res*., 2020, **14**, 546-553.

[9] S. Dutta, S. Mukherjee, O. T. Qazvini, A. K. Gupta, S. Sharma, D. Mahato, R. Babarao and S. K. Ghosh, Three-in-One C_2H_2-Selectivity-Guided Adsorptive Separation across an

Isoreticular Family of Cationic Square-Lattice MOFs, *Angew. Chem. Int. Ed*. 2022, **61**, e202114132.

[10] Y. Ye, S.Xian, H. Cui, K. Tan, L. Gong, B. Liang, T. Pham, H. Pandey, R.Krishna, P. Lan, K. Forrest, B. Space, T. Thonhauser, J. Li and S. Ma, Metal-Organic Framework Based Hydrogen-Bonding Nanotrap for Efficient Acetylene Storage and Separation, *J. Am. Chem. Soc.* 2022, **144**, 1681-1689.

[11] X. Duan, Q. Zhang, J. Cai, Y. Yang, Y. Cui, Y. He, C. Wu, R. Krishna, L. Chen and G. Qian, A new metal-organic framework with potential for adsorptive separation of methane from carbon dioxide, acetylene, ethylene, and ethane established by simulated breakthrough experiments, *J. Mater. Chem. A*, 2014, **2**, 2628-2633.

[12] G. Chang, B. Li, H. Wang, T. Hu, Z. Bao and B. Chen, Control of interpenetration in a microporous metal-organic framework for significantly enhanced C_2H_2/CO_2 separation at room temperature, *Chem. Commun.,* 2016, **52**, 3494-3496.

[13] R. Liu, Q. Liu, R. Krishna, W. Wang, C. He and Y. Wang, Water-Stable Europium 1,3,6,8-Tetrakis(4-carboxylphenyl)pyrene Framework for Efficient C_2H_2/CO_2 Separation, *Inorg. Chem*., 2019, **58**, 5089-5095.

[14] J. Gao, X. Qian, R. Lin, R. Krishna, H. Wu, W. Zhou and B. Chen, Mixed Metal-Organic Framework with Multiple Binding Sites for Efficient C_2H_2/CO_2 Separation, *Angew. Chem. Int. Ed*, 2020, **59**, 4396-4400.

[15] H. Lv, Y. Li, Y. Xue, Y. Jiang, S. Li, M. Hu and Q. Zhai, Systematic Regulation of C_2H_2/CO_2 Separation by 3p-Block Open Metal Sites in a Robust Metal-Organic Framework Platform, *Inorg. Chem.* 2020, **59**, 4825-4834.

[16] L. Z. Liu, Z. Z. Yao, Y. X. Ye, L. J. Chen, Q. J. Lin, Y. S. Yang, Z. J. Zhang, S. C. Xiang and J. Robustness, Selective Gas Separation, and Nitrobenzene Sensing on Two Isomers of Cadmium Metal-Organic Frameworks Containing Various Metal-O-Metal Chains, *Inorg. Chem.*, 2018, **57**, 12961–12968.

[17] H. Cui, Y. X. Ye, H. Arman, Z. Q. Li, A. Alsalme, R. B. Lin and L. Chen, Microporous Copper Isophthalate Framework of mot Topology for C_2H_2/CO_2 Separation, *Cryst. Growth Des.*, 2019, **19**, 5829–5835.

[18] S. Mukherjee, Y. He, D. Franz, S. Q. Wang, W. R. Xian, A. A. Bezrukov, B. Space, Z. Xu,

J. He and M. J. Zaworotko, Halogen-C_2H_2 Binding in Ultramicroporous Metal-Organic Frameworks (MOFs) for Benchmark C_2H_2/CO_2 Separation Selectivity, *Chem.-Eur. J*., 2020, **26**, 4923–4929.

[19] Y. Li, Y. Wang, Y. Xue, H. Li, Q. Zhai, S. Li, Y. Jiang, M. Hu and X. Bu, Ultramicroporous Building Units as a Path to Bi-microporous Metal-Organic Frameworks with High Acetylene Storage and Separation Performance, *Angew. Chem. Int. Ed*. 2019, **58**, 13590-13595.

[20] Y. T. Li, J. W. Zhang, H. J. Lv, M. C. Hu, S. N. Li, Y. C. Jiang and Q. G. Zhai, Tailoring the Pore Environment of a Robust Ga-MOF by Deformed $[Ga_3O(COO)_6]$ Cluster for Boosting C_2H_2 Uptake and Separation, *Inorg. Chem.*, 2020, **59**, 10368 – 10373.

[21] J. W. Zhang, M. C. Hu, S. N. Li, Y. C. Jiang, P. Qu and Q. G. Zhai, Assembly of $[Cu_2(COO)_4]$ and $[M_3(\mu_3\text{-}O)(COO)_6]$ (M = Sc, Fe, Ga, and In) building blocks into porous frameworks towards ultra-high C_2H_2/CO_2 and C_2H_2/CH_4 separation performance, *Chem. Commun.*, 2018, **54**, 2012-2015.

[22] J. Pei, K. Shao, J. X. Wang, H.-M. Wen, Y. Yang, Y. Cui, R. Krishna, B. Li and G. D. Qian, A Chemically Stable Hofmann-Type Metal−Organic Framework with Sandwich-Like Binding Sites for Benchmark Acetylene Capture, Adv. Mater., 2020, **32**, 1908275.

[23] Z. Niu, X. Cui, T. Pham, G. Verma, P. C. Lan, C. Shan, H. Xing, K. A. Forrest, S. Suepaul, B. Space, A. Nafady, A. M. Al-Enizi and S. Ma, A MOF-based Ultra-Strong Acetylene Nano-trap for Highly Efficient C_2H_2/CO_2 Separation, *Angew. Chem. Int. Ed*. 2021, **60**, 5283-5288.

[24] H. Zeng, M. Xie, Y. L. Huang, Y. F. Zhao, X. J. Xie, J. P. Bai, M. Y. Wan, R. Krishna, W. G. Lu and D. Li, Induced Fit of C_2H_2 in a Flexible MOF Through Cooperative Action of Open Metal Sites, *Angew. Chem. Int. Ed*., 2019, **58**, 8515-8519.

[25] O. T. Qazvini, R. Babarao and S. G. Telfer, Multipurpose Metal-Organic Framework for the Adsorption of Acetylene: Ethylene Purification and Carbon Dioxide Removal, *Chem. Mater.*, 2019, **31**, 4919-4926.

[26] J. Reynoids, K. Walsh, B. Li, P. Kunal, B. Chen and S. Humphrey, Highly selective room temperature acetylene sorption by an unusual triacetylenic phosphine MOF, *Chem. Commun.,* 2018, **54**, 9937-9940.

[27] H. Li, C. Liu, C. Chen, Z. Di, D. Yuan, J. Pang, W. Wei, M. Wu and M. Hong, An Unprecedented Pillar-Cage Fluorinated Hybrid Porous Framework with Highly Efficient Acetylene Storage and Separation, *Angew. Chem. Int. Ed.* 2021, **60**, 7547.

[28] F. Luo, C. S. Yan, L. L. Dang, R. Krishna, W. Zhou, H. Wu, X. L. Dong, Y. Han, T. L. Hu, M. O'Keeffe, L. L. Wang, M. B. Luo, R. B. Lin and L. Chen, UTSA-74: A MOF-74 Isomer with Two Accessible Binding Sites per Metal Center for Highly Selective Gas Separation, *J. Am. Chem. Soc.*, 2016, **138**, 5678-5684.

[29] J. G. Duan, W. Q. Jin and R. Krishna, Natural Gas Purification Using a Porous Coordination Polymer with Water and Chemical Stability, *Inorg. Chem*., 2015, **54**, 4279-4284.

[30] Q. B. Dong, Y. N. Guo, H. F. Cao, S. N. Wang, R. Matsuda and J. G. Duan, Accelerated C_2H_2/CO_2 Separation by a Se-Functionalized Porous Coordination Polymer with Low Binding Energy, *ACS Appl. Mater. Interfaces,* 2020, **12**, 3764-3772.

[31] L. Zhang, C. Zou, M. Zhao, K. Jiang, R. B. Lin, Y. B. He, C. D. Wu, Y. J. Cui, B. Chen and G. D. Qian, Doubly Interpenetrated Metal-Organic Framework for Highly Selective C_2H_2/CH_4 and C_2H_2/CO_2 Separation at Room Temperature, *Cryst. Growth Des.,* 2016, **16**, 7194-7197.

[32] W. D. Fan, S. Yuan, W. J. Wang, L. Feng, X. P. Liu, X. R. Zhang, X. Wang, Z. X. Kang, F. N. Dai, D. Q. Yuan, D. F. Sun and H. C. Zhou, Optimizing Multivariate Metal-Organic Frameworks for Efficient C_2H_2/CO_2 Separation, *J. Am. Chem. Soc*., 2020, **142**, 8728-8737.

[33] L. Zhang, K. Jiang, Y. Li, D. Zhao, Y. Yang, Y. Cui, B. Chen and G. Qian, Microporous Metal-Organic Framework with Exposed Amino Functional Group for High Acetylene Storage and Excellent C_2H_2/CO_2 and C_2H_2/CH_4 Separations, Cryst. Growth Des., 2017, **17**, 2319-2322.

[34] T. Xu, Z. Jiang, P. Liu, H. Chen, X. Lan, D. Chen, L. Li and Y. He, Immobilization of Oxygen Atoms in the Pores of Microporous Metal-Organic Frameworks for C_2H_2 Separation and Purification, *ACS Appl. Nano Mater.,* 2020, **3**, 2911-2919.

[35] H. S. Scott, M. Shivanna, A. Bajpai, D. G. Madden, K. J. Chen, T. Pham, K. A. Forrest, A. Hogan, B. Space, J. J. Perry and M. J. Zaworotko, Highly Selective Separation of C_2H_2 from CO_2 by a New Dichromate-Based Hybrid Ultramicroporous Material, *ACS Appl. Mater. Interfaces*, 2017, **9**, 33395-33400.

[36] L. Zhang, K. Jiang, J. Zhang, J. Pei, K. Shao, Y. Cui, Y. Yang, B. Li, B. Chen and G. D. Qian, Low-Cost and High-Performance Microporous Metal-Organic Framework for Separation of Acetylene from Carbon Dioxide, *ACS Sustainable Chem. Eng*. 2019, **7**, 1667-1672.

[37] H. Wen, C. Liao, L. Li, L. Yang, J. Wang, L. Huang, B. Li, B. Chen and J. Hu, Reversing C_2H_2-CO_2 adsorption selectivity in an ultramicroporous metal-organic framework platform, *Chem. Commun.*, 2019, **55**, 11354-11357.

[38] Y. Zhang, L. Yang, L. Wang, S. Duttwyler and H. Xing, A Microporous Metal-Organic Framework Supramolecularly Assembled from a Cu^{II} Dodecaborate Cluster Complex for Selective Gas Separation, *Angew. Chem. Int. Ed.* 2019, **58**, 8145-8150.

[39] Y. Zhang, L. Yang, L. Wang and H. Xing, Pillar iodination in functional boron cage hybrid supramolecular frameworks for high performance separation of light hydrocarbons, *J. Mater. Chem. A*, 2019, **7**, 27560-27566.

[40] Y. Zhang, J. Hu, R. Krishna, L. Wang, L. Yang, X. Cui, S. Duttwyler and H. Xing, Rational Design of Microporous MOFs with Anionic Boron Cluster Functionality and Cooperative Dihydrogen Binding Sites for Highly Selective Capture of Acetylene, *Angew. Chem. Int. Ed.*, 2020, **59**, 17664-17669.

[41] Y. Zhang, L. Wang, J. Hu, S. Duttwyler, X. Cui and H. Xing, Solvent-dependent supramolecular self-assembly of boron cage pillared metal-organic frameworks for selective gas separation, *CrystEngComm*, 2020, **22**, 2649-2655.

[42] L. Wang, W. Sun, Y. Zhang, N. Xu, R. Krishna, J. Hu, Y. Jiang, Y. He and H. Xing, Interpenetration Symmetry Control Within Ultramicroporous Robust Boron Cluster Hybrid MOFs for Benchmark Purification of Acetylene from Carbon Dioxide, *Angew. Chem. Int. Ed*. 2021, **60**, 22865-22870.

[43] W. Sun, Y. Jin, Y. Wu, W. Lou, Y. Yuan, S. Duttwyler, L. Wang and Y. Zhang, A new boron cluster anion pillared metal organic framework with ligand inclusion and its selective acetylene capture properties, *Inorg. Chem. Front*., 2022, DOI: 10.1039/d2qi00890d.

[44] R. Lin, L. Li, H. Wu, H. Arman, B. Li, R. G. Lin, W. Zhou and B. Chen, Optimized Separation of Acetylene from Carbon Dioxide and Ethylene in a Microporous Material, *J. Am. Chem. Soc.*, 2017, **139**, 8022-8028.

[45] W. Sun, J. Hu, Y. Jiang, N. Xu, L. Wang, J. Li, Y. Hu, S. Duttwyler and Y. Zhang, Flexible molecular sieving of C_2H_2 from CO_2 by a new cost-effective metal organic framework with intrinsic hydrogen bonds, *Chem. Eng. J*, 2022, **439**, 135745.

[46] J. Wang, Y. Zhang, Y. Su, X. Liu, P. Zhang, R. Lin, S. Chen, Q. Deng, Z. Zeng, S. Deng and B. Chen, Fine pore engineering in a series of isoreticular metal-organic frameworks for efficient C_2H_2/CO_2 separation, *Nat Commun*, 2022, **13**, 200.

[47] Q. Dong, X. Zhang, S. Liu, R. Lin, Y. Guo, Y. Ma, A. Yonezu, R. Krishna, G. Liu, J. Duan, R. Matsuda, W. Jin and B. Chen, Tuning Gate-Opening of a Flexible Metal-Organic Framework for Ternary Gas Sieving Separation, *Angew. Chem. Int. Ed.* 2020, **59**, 22756-22762.

[48] L. Yang, L. Yan, Y. Wang, Z. Liu, J. He, Q. Fu, D. Fu, D. Liu, X. Gu, P. Dai, L. Li and X. Zhao, Adsorption Site Selective Occupation Strategy within a Metal-Organic Framework for Highly Efficient Sieving Acetylene from Carbon Dioxide, *Angew. Chem. Int. Ed.*, 2021, **60**, 4570-4574.